Received: 23 March 2023 | Revised: 25 May 2023 | Accepted: 20 June 2023

DOI: 10.1002/htj.22921

ORIGINAL ARTICLE

HEAT TRANSFER WILEY

Bio-based building components: A newly sustainable solution for traditional walls made of *Arundo donax* and gypsum

Francesco Barreca[1] | **Giuseppe Cardinali**[1] | **Alberto Barbaresi**[2] | **Marco Bovo**[2]

[1]Università Degli Studi Mediterranea di Reggio Calabria, Reggio Calabria, Italy

[2]Alma Mater Studiorum Università di Bologna, Bologna, Italy

Correspondence
Francesco Barreca, Università Degli Studi Mediterranea di Reggio Calabria, Reggio Calabria 89124, Italy.
Email: fbarreca@unirc.it

Abstract

To contribute to the use of bio-based materials in the building sector, a novel bio-based wall panel, with a high thermal performance level, is proposed in this work. The panel is based on an ancient rural technique, widely diffused in southern Italy, which makes use of *Arundo donax* L. canes combined with gypsum plaster to build walls and ceilings of rural buildings. The enhancement of the thermal capacity of these panels by means of the introduction in the canes of a natural wax oleogel (WO) is proposed in this paper. A specific experimental campaign aiming at the comparison of traditional and innovative panels was carried out to assess the enhanced thermal performance of the proposed solution. The maximum value of heat flow absorbed from the panel with WO was 61.08 W/m^2 around a mean panel temperature of 24°C, corresponding to the melting temperature range of the WO. The panel without WO at the same temperature absorbed an incoming heat flow of 34.64 W/m^2 which is about 57% of the panel with WO. The panel with WO released at a temperature of about 27.5°C, a heat flow of 43.42 W/m^2. At the same temperature of about

27.5°C, the panel without WO released a heat flow of 34.38 W/m^2 which is about 80% that of the panel with WO. The results highlighted that the addition of natural WO has enhanced the thermal capacity of the panel facilitating heat dissipation through the borders. These characteristics make the panel a suitable component for internal partitions of controlled temperature zones such as residential rooms, storage food areas, livestock buildings, and where it is necessary to obtain a constant environmental temperature. In particular, the null or low toxicity of the panel's materials allows for partition use, also in hygienically safe environments.

KEYWORDS
biological components, biotechnology, buildings, phase change materials/systems

1 | INTRODUCTION

The building sector is responsible for about 40% of global emissions and 35% of primary energy demand.[1] The use of coal and natural gas for heating, cooling, cooking, or the use of electricity (when the electricity production remains carbon-intensive) produces a high level of undesired emissions. The main goal of the European Green Deal[2] is to obtain an economy with net-zero greenhouse gas emissions by 2050. The building industry plays an important role in achieving the decarbonization of the global economy through improvements in energy efficiency to reduce energy demand, by reducing the use of materials and their embodied carbon, and by supporting the adoption of distributed low-carbon and renewable energy generation. An important goal of the European Green Deal is to improve the well-being and health of citizens and future generations by providing fresh air, clean water, healthy soil, biodiversity, and renovated energy-efficient buildings. The priorities below are the main aims identified by the stakeholders to deliver zero-emission, efficient, and resilient buildings by 2050:

- prioritizing high-efficiency standards and optimizing design processes, design strategies, codes, and labels to build new high-energy performance buildings.
- accelerating actions on existing building retrofits to enhance their thermal performance.
- promoting the use of low-carbon materials to develop efficiency in the manufacturing of innovative components to reduce the embodied carbon over a building's whole life cycle.

The construction of net-zero energy and zero-carbon buildings by 2050 has become a key part of the global decarbonization strategy. New buildings will be a major source of emissions in the future, especially in emerging countries. The global population is expected to rise to 8.5 billion by 2030 and up to 9.7 billion by 2050.[3] The research community, promoting the creation

of more sustainable new buildings, is studying the performance of new building envelopes, including conduction and radiation heat transfer through optimized bio-based materials, design strategies, and the use of vegetation, as in the example of green roofs. The insulation of the building envelope is one of the main components that should be specifically targeted for cold locations. The insulation performance of the envelope is usually determined by thermal conductivity (λ), which is used to express how much heat will be transferred through a given thickness of a particular material. The lower the λ value is, the more the material is a thermal insulator. The benefits of insulation must be evaluated over the whole life cycle as traditional insulating materials have a high level of embodied carbon. The building code could affect the designer's choices of high thermal performance sustainable materials. In developed countries, most buildings are already built and, for these economies, the retrofitting of the envelope of existing buildings is the most important strategy to reduce carbon emissions. Besides, the insulation of the envelope is very important in these buildings. It is important to note that insulation is a priority in cold climates and is most effective over larger surface area components (i.e., roofs for flat buildings and walls for tall buildings), but in hot climates, it is very important to use high thermal capacity materials for the whole building envelope.[4,5] Over the past few years, a new approach has been adopted to achieve a thermal flow reduction through the envelope, this approach takes advantage of phase change materials (PCMs). These materials release or absorb large amounts of latent heat at each phase transition (from solid to liquid and vice versa). The materials used in buildings play a key role in sustainability, in fact, the construction and demolition of buildings account for around one-third of global material consumption and waste generation in the EU.[6] The greenhouse gas emissions and energy consumption are linked to every phase of the life cycle of materials, from extraction or harvesting, to manufacture, transport, construction, use, and demolition. Among the building materials, concrete, metals, bricks, and wood are some of the major emitters of CO_2.

Emissions from the production of building materials and building construction are largely driven by concrete and steel manufacturing,[7] and their growth in use is a major driver of building-related embodied carbon emissions. Building design and type, such as high-rise towers, have resulted in increased demand for steel and concrete, though such buildings may have a longer lifespan as a result. Globally, the building construction sector accounts for approximately 50% of the demand for cement and 30% of steel.[8] These factors show the importance of extending the lifetime of buildings and reducing the use of cement and replacing them with materials that have lower embodied carbon. The use of bio-based building materials can drastically reduce CO_2 emissions due to the low energy used in the extraction and construction stages.[9,10] On the other hand, the use of bio-based materials was very common in traditional architecture, particularly in rural contexts, as a way of taking advantage of the resources available in the proximity of the building site. Today, traditional ways of building have assumed a new significance as good examples of sustainable architecture.

Unfortunately, the use of natural materials is not still largely diffuse in the worldwide building industries mainly due to some factors as, for example:

- difficulty in standardizing building component production;
- difficulty in carrying out a LCA comparison with conventional materials, making it challenging to use this analysis to extract environmental management recommendations or to determine design change requirements;
- the technical performances of bio-based materials are not often compared to conventional building materials;

- absence of data about the long-term behavior of natural materials especially with regard to durability request;
- the use of bio-based materials can increase the complexity of the industrial process.

To address these gaps and to contribute to the use of bio-based materials in the building sector, a novel bio-based wall panel, with a high thermal performance level, is proposed in this work. To diffuse the use of bio-based materials in the building sector, it is important to understand the technical performance of the materials in real conditions of use. In this work, a detailed experimental analysis was conducted to evaluate the thermal performance of a bio-based panel for the building industry. Tests were performed simulating real-world conditions such as dynamic temperature variation and the main thermal parameters were estimated to compare the performance behavior of the traditional solution and the novel proposed solution. The new solution was developed to enhance the thermal performance of the traditional one while still maintaining the bio-based nature. The panel is based on an ancient rural technique, widely diffused in southern Italy, which makes use of *Arundo donax* L. (A.d.) canes combined with gypsum plaster to build walls and ceilings of rural buildings.[11,12] These building components have good thermal insulation combined with lightweight and easy construction processes.[13,14] The enhancement of the thermal capacity of these panels by means of the introduction in the canes of a natural wax oleogel (WO), that is, a gelator that dissolves in oil upon heating and crystallizes upon cooling absorbing and releasing heat, is proposed in this paper (see Figure 1). A specific experimental campaign, aiming at the comparison of traditional and innovative panels was carried out to assess the enhanced thermal performance of the proposed solution.

2 | MATERIALS AND METHODS

2.1 | Characteristics of A.d.

A.d. is a rhizomatous perennial grass species native to East Asia and belongs to the Poaceae family. Thanks to its adaptability to a wide range of climatic habitats, it has also been cultivated in South Europe, Northern Africa, and Saudi Arabia. Then, in the past centuries, it was introduced in the United States and Australia and soon became so widespread, that it was considered an invasive alien species[15,16] which caused uncontrolled fires, an obstruction of waterways,[17] as well as being an antagonist of other plant species.[18] This led the administrations of some countries to promote specific programs of control and eradication.

This invasive plant replaced native species on several portions of European riverbanks, affecting the morphology of the river and causing severe problems such as blocking the flow of the river. Its complete eradication is difficult to carry out, and control strategies have been developed. Also, the control of its propagation is a very expensive task for river managers. Moreover, the processing of the removing A.d. culm requires a lot of effort and high costs. Farmers often consider its presence as damaging to agriculture because it subtracts soil from the more profitable plants.

On the other hand, in other parts of the world A.d. was utilized in the past as a construction material by various populations. In fact, thanks to their lightness and strength, A.d. stems have been employed in the past for the realization of building components.[19] A paradigmatic example of designing with reed are the Sumerian mudhif[20] constructions built entirely of reed,

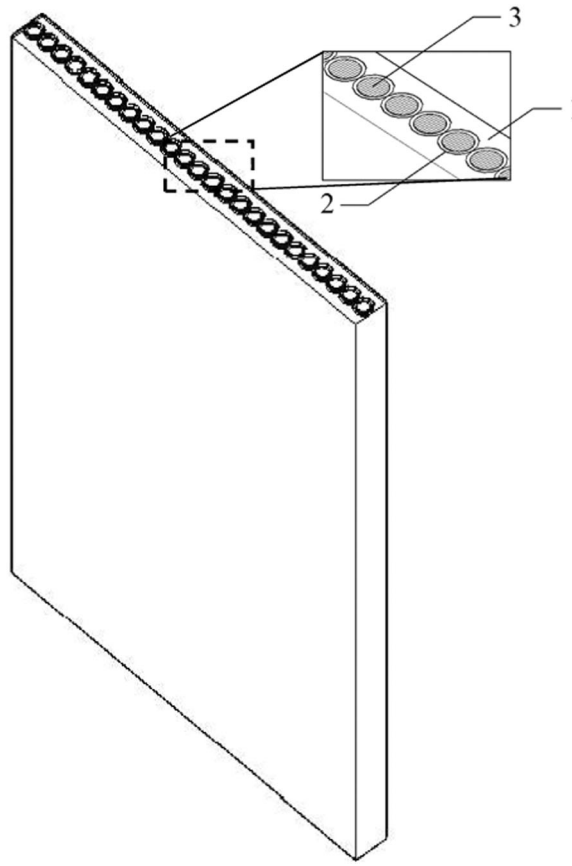

FIGURE 1 The proposed wall panel combining (1) gypsum plaster, (2) *Arundo donax* canes, and (3) wax oleogel filler.

TABLE 1 LORD parameters and results carried out.

Panel	H 1–2 ($W m^{-2} K^{-1}$)	H 2–3 ($W m^{-2} K^{-1}$)	H 3–4 ($W m^{-2} K^{-1}$)	C2 (MJ/K)	C3 (MJ/K)
GC	9.72	6.17	2000.0	0.0251	0.0158
GCO	1994.97	7.87	8.71	0.0172	0.0362

and dating back 5000 years. Some peasant populations have based most of their productive activity on the cultivation and processing of this plant. A.d. finds many and varied uses in the vernacular and rural architecture of the Mediterranean basin, and in particular of many Italian regions: in the building envelope, in internal partitions (panels and walls), in the roofing system, and in structural elements such as beams or panels, made in situ, usually consisting of parallel reeds woven across perpendicular elements of cane or, more commonly, with mortar, plaster, or raw earth.[21,22] Interesting modern re-visitations of the ancient techniques have been recently proposed such as those by Canyaviva[23] based on arches made with reeds held together in bundles. The mechanical properties of A.d. canes are comparable to those of Bamboo (see Table 1) and due to their bigger culm dimensions (i.e., diameter and thickness), they are often

used for structural aims. Due to the internal cavity, the A.d. culms have good thermal insulation and lightweight properties, so they were used for shelter, and to build walls, partitions, and ceilings in some Mediterranean areas.[24] There are several examples of building components made of A.d. cane, often in combination with raw earth, lime, gypsum, and other coating materials, essential to obtain a plane regular surface. In particular, gypsum components are widely used in the building industry for such things as boards, which it is possible to assemble in a dry and fast way and can be used to easily construct the surface of a large wall. Gypsum bricks are less common than gypsum boards but are used for indoor walls with a high thermal mass and with high impact resistance. Disadvantages can be found in the longer assembling time and the final heavier weight of the boards. The thick gypsum panels with A.d. canes were only used for a short time, although they only took a short time to assemble. This paper proposes a gypsum panel with a middle layer of juxtaposed canes of A.d., where each cane is filled with a natural oleogel material. The canes allow the material to liquify, when the temperature increases, without running out of the panel and solidify when the temperature decreases.

2.2 | Phase change materials

The use of PCM as thermal energy storage (TES) has been widely applied in various fields, such as cold chain logistics,[25,26] electric energy storage,[27,28] photovoltaic energy production,[29] HVAC systems[30] as well as in other sectors of the building industry.[31,32] The use of TES is intended to save energy and release it when needed. For this, it is fundamental to carry out a proper design of the PCM system, identifying the most suitable melting temperature by choosing the right material. The PCM could be made of inorganic (e.g., hydrated salts) or organic (e.g., paraffin) substances. Research has recently been looking for new natural substances to use to enhance the safety of the environment and the health of the building occupants.[33] Some natural materials show behavior similar to PCM during the heating and cooling phases. In particular, some natural oleogels, which consist of low concentrations of gelators that dissolve in oil upon heating, and crystallize upon cooling, form a thermoreversible network of crystals that encases liquid oil and provides a semisolid texture absorbing and releasing heat during the melting and the crystallization phases.[34] Winkler-Moser et al.[25] studied an oleogel made with soybean oil, based on natural waxes, specifically beeswax (BW) and candelilla wax (CLW) mixture.[23] They analyzed the interactions of these WOs, in terms of crystallization and melting properties, crystal morphology, solid fat content, and gel firmness. They studied the thermal properties of this WO and different combinations of CLW and BW were analyzed. The results highlighted the effect of wax percentage on firmness, onset temperature (T_{on},°C), peak maximum temperature (T_p,°C), and enthalpies (ΔH, J/g) for all major crystallizations and melting peaks related to the wax portions of the oleogels.

In this study, a binary mixture of 5% of BW and CLW, with a ratio of 20:80 CLW:BW with soybean oil to produce a WO was chosen, and its effect was tested with the A.d. and gypsum panel. The thermal profile of the WO was selected according to Winkler-Moser et al.[25] This ratio of mixture between CLW to BW for the WO was chosen because this ratio showed an onset melting temperature close to 22.45°C, which is considered a suitable indoor temperature for a comfortable home.

2.3 | The experimental campaign

2.3.1 | Thermal panel analysis

A preliminary thermal test was carried out on a wall panel sample composed of gypsum and canes (named GC sample) without the WO filler. Then, a second thermal test has been carried out with WO material inside the canes (named GCO test) to analyze the behavior of the panel with the presence of WO material.

A 80 cm × 100 cm × 5 cm (width × height × thickness) sample panel was built. A semifluid mix of powder gypsum (e.g., calcium sulfate dihydrate) with a 4:1 proportion to water was poured into a wooden framework. A panel of juxtaposed A.d. culms with an average diameter of 2 cm, average thickness of 0.25 cm, and a length of 80 cm was placed at the center of the semifluid mass (see Figure 2).

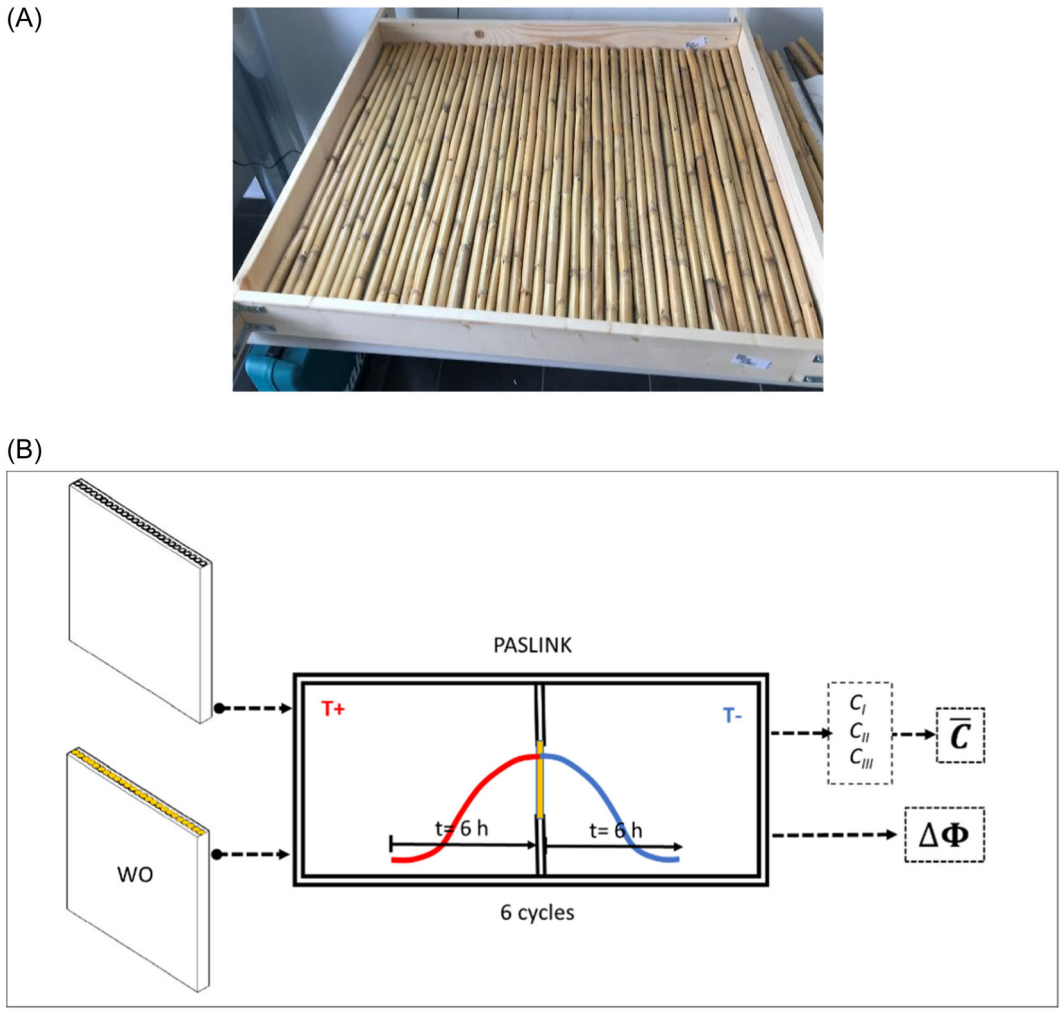

FIGURE 2 Experimental campaign. (A) Preparation of the sample with *Arundo donax* culms layer inside the gypsum panel. (B) Flow chart of the experimental campaign.

The panels were dried in a room with a controlled temperature equal to 35°C and relative humidity of 60% for 7 days. At the end of the drying period, a humidity of 10% was measured on the surface. The dried gypsum A.d. panel was placed in an indoor climate cell (PASLINK) to obtain the thermal characteristics of the panel under dynamic thermal conditions.

In particular, a variable air thermal gradient higher than 10°C was created between the two faces of the panel. With a couple of PT 100 sensors, the surface temperature was measured. A couple of heat flow sensors was used to measure the incoming and outcoming heat flow on each face of the panel (see Figure 3).

Relative humidity and temperature air sensors were installed in each cell. An infrared heater was used to heat the hot cell and to simulate the dynamic thermal conditions for a period of 72 h. The heater was turned on and off every 6 h, therefore six heating and cooling cycles were alternated in the cell. The thermal values were surveyed and stored every 15 min using a programmable data logger (LSI LASTEM) (see Figure 4).

2.3.2 | Thermal conductance evaluation

The evaluation of the thermal conductance using a heat flow meter apparatus needs a careful and correct data analysis. Many factors can affect this evaluation which is based on the analysis of the measured data and on post-processing methods. In this study, the following three different data analysis methods, available in the scientific literature, were applied: the mean progressive method, the black box method, and the Lord technique.[35]

The mean progressive method suggested by the ISO 9869[36] consists of the calculation of the conductance by means of flow and temperature values considering all previous instants. This International Standard Test describes the heat flow meter method for the measurement of the thermal transmission properties of plane building components primarily consisting of opaque layers perpendicular to the heat flow and having no significant lateral heat flow. A thermal

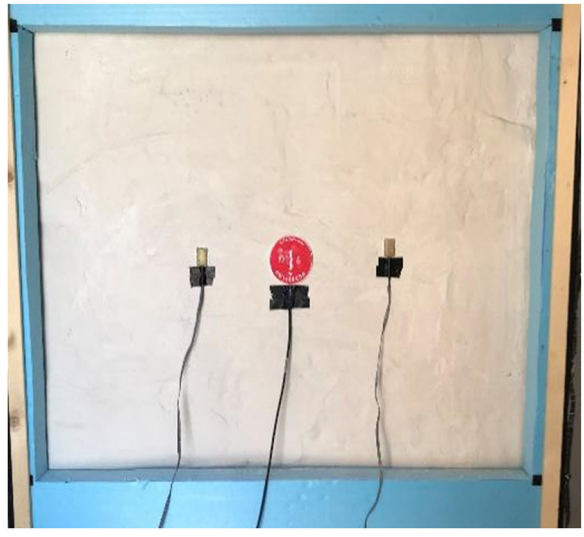

FIGURE 3 Sample panel with heat flow meter and temperature sensors mounted for the thermal tests.

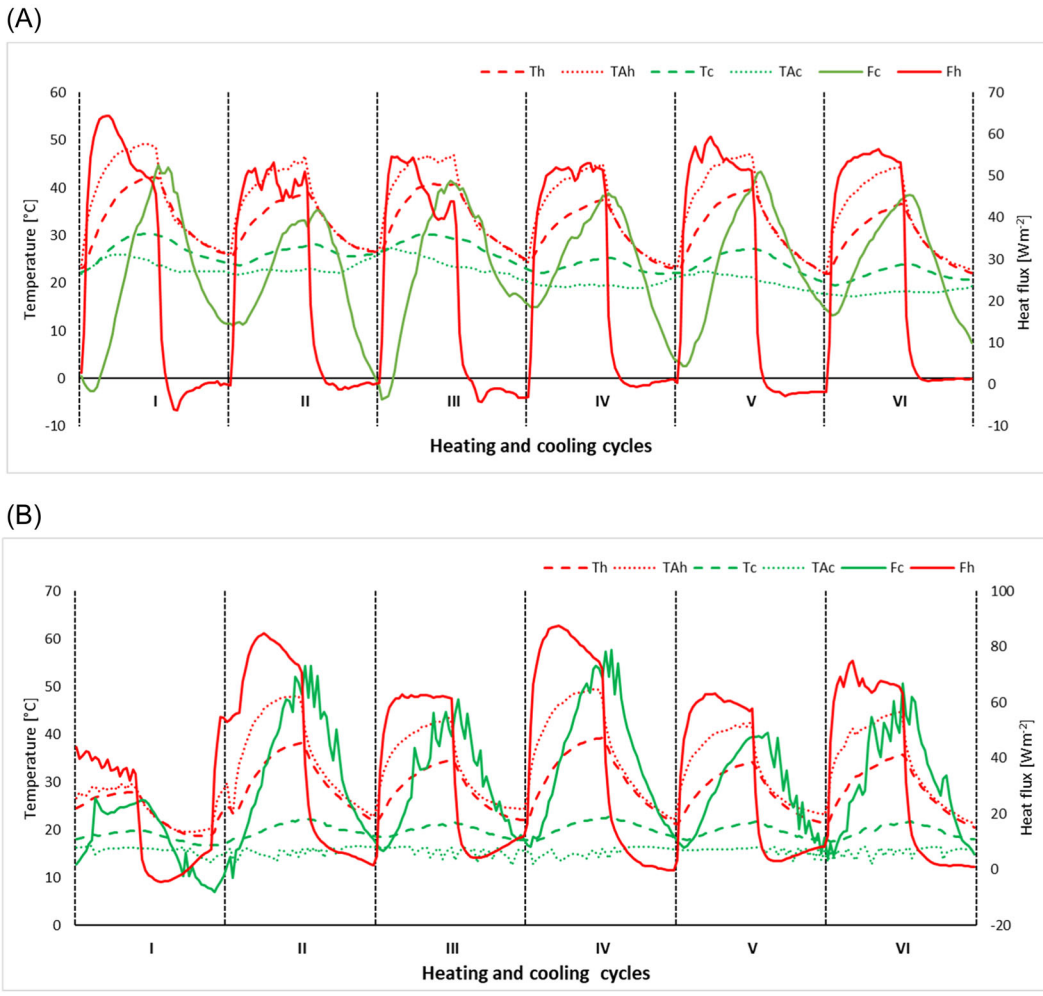

FIGURE 4 Thermal characteristics of the tested panels (T_h, temperature of hot side; T_{Ah}, air temperature of the hot cell; T_c, temperature of cold side; T_{Ac}, air temperature of the cold cell; F_h, heat flow measured on the hot side; and F_c, heat flow measured on the cold side). (A) Without WO (B) with WO.

infrared camera allowed verification of the homogeneity of sample surface temperatures as well as possible heat losses or hidden sources of thermal radiation (see Figure 5).

After 72 h of measurements and after checking the respect of the conditions prescribed by ISO 9869 (e.g., constant difference in temperature between the hot and cold spaces higher than 10°C and a heat flow >5 W/m^2), the instantaneous conductance value was calculated by means of Equation (1).

$$C_t = \frac{\phi(t)}{T_h(t) - T_c(t)}, \tag{1}$$

where C_t is the conductance at time t (W m^{-2} K^{-1}), $\phi(t)$ is the instantaneous density of heat flow rate at time t (W m^{-2}), $T_h(t)$, and $T_c(t)$ are the instantaneous temperatures on the hot and cold surface of the sample at time t (K), respectively.

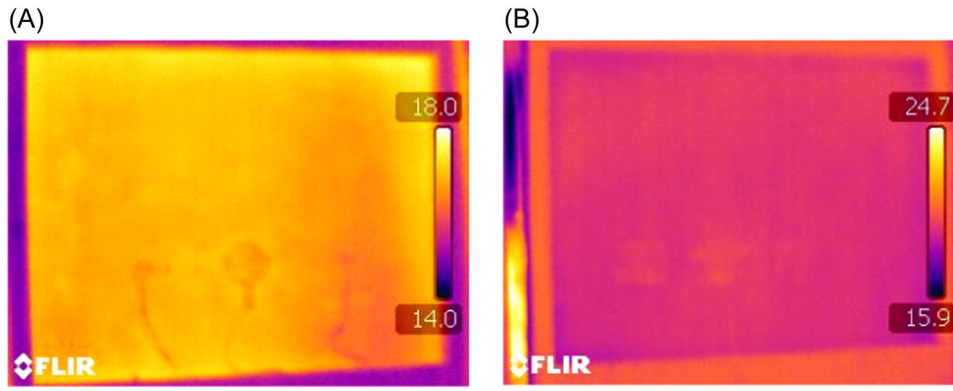

FIGURE 5 Infrared image of the panel. (A) Cold side. (B) Hot side.

The procedure used is the mean progressive method, which implies the calculation of parameters as mean values of the n measurements taken at the previous times. Therefore, Equation (1) can be rewritten as follows:

$$C_{\mathrm{A}} = \frac{\bar{\phi}(t)}{\bar{T}_{\mathrm{h}}(t) - \bar{T}_{\mathrm{c}}(t)}, \tag{2a}$$

$$\bar{T}_{\mathrm{h}}(t) = \frac{1}{n}\sum_{i=1}^{n} T_{\mathrm{h}}(t_i), \tag{2b}$$

$$\bar{T}_{\mathrm{c}}(t) = \frac{1}{n}\sum_{i=1}^{n} T_{\mathrm{c}}(t_i), \tag{2c}$$

$$\bar{\phi}(t) = \frac{1}{n}\sum_{i=1}^{n} \phi(t_i), \tag{2d}$$

where C_A is the final value of the conductance, calculated by the average method.

The progressive average of the values enabled the limiting of the influence of the system transient periods and of the peak heat values caused by the effect of thermal storage or possible anomalies of the system.

The black box method[37] does not require the knowledge of the physical panel components but it needs only the knowledge of input data (i.e., cold and hot surface temperatures) and output data (i.e., heat flow). The physical characteristics of the panel can be obtained by means of a statistical method applied to the input data providing the thermal conductance value. This method is based on the solution of Equation (3):

$$\begin{aligned}\bar{\bar{\phi}}(t_n) + a_1\phi(t_{n-1}) + \ldots + a_{na}\phi(t_{n-na}) = {} & b_{1,1}T_i(t_{n-1}) + \ldots + b_{1,nb1}T_i(t_{n-nb1}) \\ & + b_{2,1}T_o(t_{n-1}) + \ldots + b_{2,nb2}T_o(t_{n-nb2}),\end{aligned} \tag{3}$$

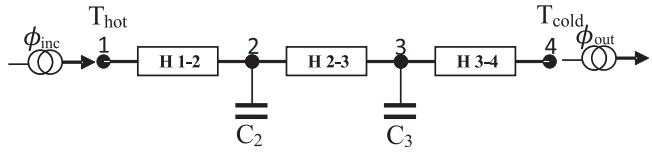

FIGURE 6 RC-model of the LORD method.

where $\bar{\bar{\phi}}(t_n)$ is the calculated heat flow value; $\phi(t_n)$ is the measured heat flow value; $T_i(t)$ is the inside temperature at time t; $T_e(t)$ is the outside temperature at time t; $\phi(t)$ is the heat flow at time t; and a_1, b_1, and b_2 are unknown coefficients.

It is expected that, at some time, the flow varies linearly from the flow value in the previous *na* steps, from the inside temperature value in the previous *nb1* steps, and from the outside temperature value in the previous *nb2* steps. It is possible to calculate the a_1, b_1, and b_2 coefficients that minimize the quadratic deviation between the calculated flux value and the measured flux value (4).

$$\sum_n (\bar{\bar{\phi}}(t_n) - \phi(t_n))^2. \tag{4}$$

Finally, the Lord method[38] assumes a one-dimensional heat flow. The technique used is the well-known lumped parameter modeling, which describes the thermal system as an electrical analog to a resistance–capacity (RC) network. The RC-model shown in Figure 6 represents the thermophysical behavior of the tested panels. In particular, the sample was schematized by two internal nodes (i.e., 2 and 3) and by two edge nodes (i.e., 1 and 4). Resistances H 1–2, H 2–3, and H 3–4 represent heat conductance, while capacities C2 and C3 represent the overall heat capacity of the sample. Node 1 was associated with the values of the flows (incoming) and temperatures measured on the hot side of the sample, while Node 4 was associated with the values of the flows (outcoming) and temperatures measured on the cold side of the panel. The software LORD[39] solves the system that considers the values measured during the transient period. Particularly, the temperature measured at Node 4 and the flow measured at Node 1 were considered as output values for the correction of the calculated values. By the statistical analysis of the deviations between the model and the measured output data, the values of the parameters are progressively adjusted to improve the final results.

By the statistical analysis of the deviations between the model and the measured output data, the values of the parameters are progressively adjusted to improve the final results. The application of the iterative procedure to different panel configurations carried out provides the values reported in Table 1.

3 | RESULTS

The application of the three different methods described in the above subsection provided the final conductance values summarized in Table 2, for the two different panel typologies. As shown in the table, the three values computed with three different methods are rather similar, and in general, as expected, the conductance values of the specimen with canes filled by WO are higher than the values provided by the wall typology with empty canes.

TABLE 2 Conductance values obtained by the application of the three different methods on the two different panels and their mean values.

Panel	Mean progressive method ($W\,m^{-2}\,K^{-1}$)	Black box method ($W\,m^{-2}\,K^{-1}$)	LORD method ($W\,m^{-2}\,K^{-1}$)	Mean value ($W\,m^{-2}\,K^{-1}$)
GC	3.75	3.92	3.77	3.81
GCO	4.08	3.99	4.13	4.07

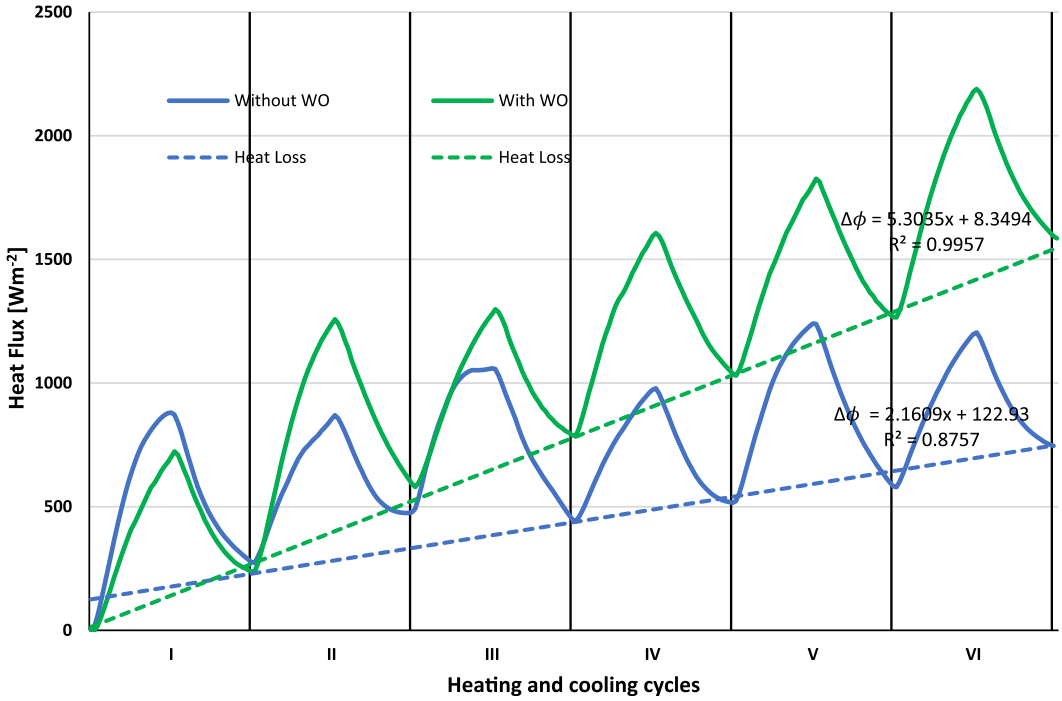

FIGURE 7 Sum of the differences of incoming and outcoming heat flow from the panels with and without WO. The dashed line represents the trend of the heat flow loss from the panel.

Controlling heat transfer and managing heat flows in a building is essential to ensure the thermal comfort of occupants, save energy, and improve sustainability. Thermal conductance is not the only parameter that defines the thermal performance of the building envelope. The study of the heat flow behavior through the building envelope is very important in non-steady-state thermal conditions and characterizes the thermal building performance. Specific tests were carried out to evaluate the heat transfer through the tested panels. These tests were carried out for 3 days (i.e., for 72 h) by means of the PASLINK apparatus.[39] Six cycles of heating and cooling to copy non-steady thermal conditions have been considered. Then, the sum of the difference of incoming (ϕ_t^i) and outcoming heat flow (ϕ_t^o) measured every 15 min was calculated, for the 72 h of testing period, with Equation 5 (see Figure 7):

$$\Delta\phi_t = \sum_{t=15\,\mathrm{min}}^{t=n\cdot 15\,\mathrm{min}} \left(\phi_t^i - \phi_t^o\right). \tag{5}$$

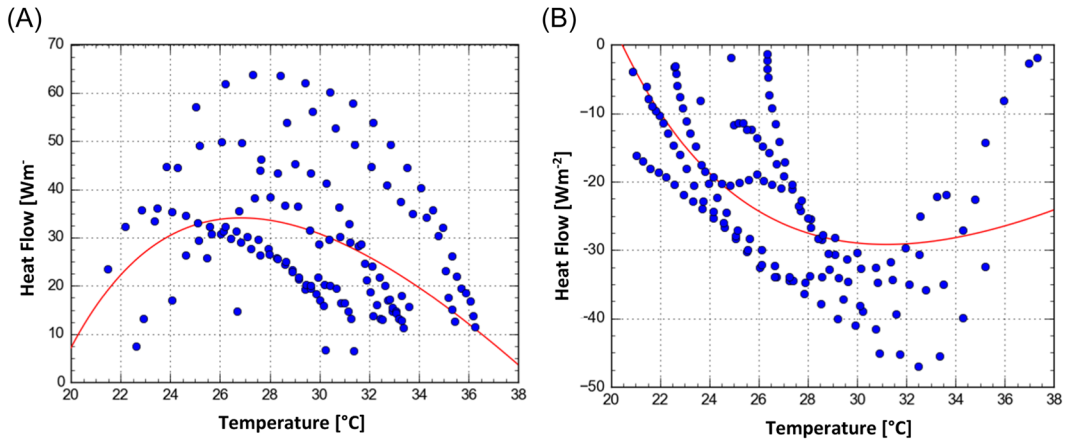

FIGURE 8 Regression curves in the graph temperature versus heat flow difference for the panel without WO. (A) Curve for phase with positive heat flow difference. (B) Curve for phase with negative heat flow difference.

On the other hand, the heat flow analysis highlighted the variation of the difference of flow to temperature variation. The sum obtained for the two different wall typologies is shown in Figure 7. The heat flow difference at the end of each cycle ($\Delta\phi_{t=12\,\mathrm{h}}$) resulted in greater than zero for both the two tested panels. So, a linear regression procedure of the heat flow residue, for each panel, was considered. The equations of the two linear regressors are

$$\Delta\phi = 2.\,1609x + 122.\,93 \tag{6}$$

and

$$\Delta\phi = 5.3035x + 8.3494, \tag{7}$$

respectively, for the panel with WO and the panel without WO. The value of the coefficient of determination R^2 is in the two cases, respectively, equal to 0.99 and 0.88.

Furthermore, a regression analysis was carried out by means of the CurveExpert Professional[40] to evaluate the existing correlation between the heat flow difference exchanged by the panel and the internal temperature calculated as the mean temperature value of both panel sides. The measured positive and negative heat flow differences and the corresponding temperatures for all periods of the test were considered for each panel. The resulting data found the best-fitting curves. For all the best-fitting curves, the "heat capacity" model was adopted. It was expressed in the equation form: $y = a + bx + cx^{-2}$. These results are shown in Figures 8 and 9. For the test without WO, the equation coefficients for the phase with positive heat flow difference are $a = 311.15$; $b = -6.88$; $c = -6580.39$, and the correlation coefficient is $R = 0.46$. The equation coefficients for phase with negative heat flow difference are $a = -166.68$; $b = 2.94$; $c = 44{,}594.69$ and the correlation coefficient is $R = 0.60$. For the test with WO, the equation coefficients for phase with positive heat flow difference are $a = 330.24$; $b = -8.38$; $c = -51{,}307.64$, and the correlation coefficient is $R = 0.49$. The equation coefficients for phase with negative heat flow difference are $a = 311.14$; $b = -6.88$; $c = -66580.39$, and the correlation coefficient is $R = 0.84$.

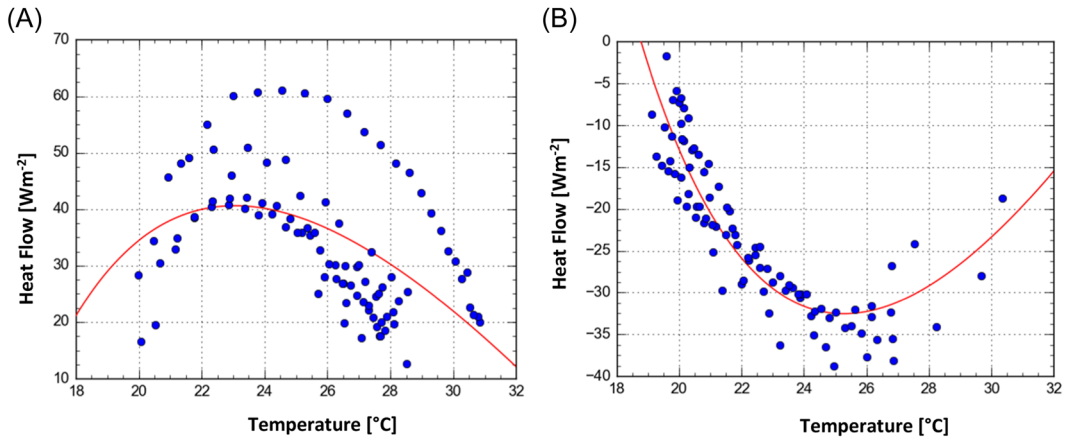

FIGURE 9 Regression curves in the graph temperature versus heat flow difference for the panel with WO. (A) Curve for phase with positive heat flow difference. (B) Curve for phase with negative heat flow difference.

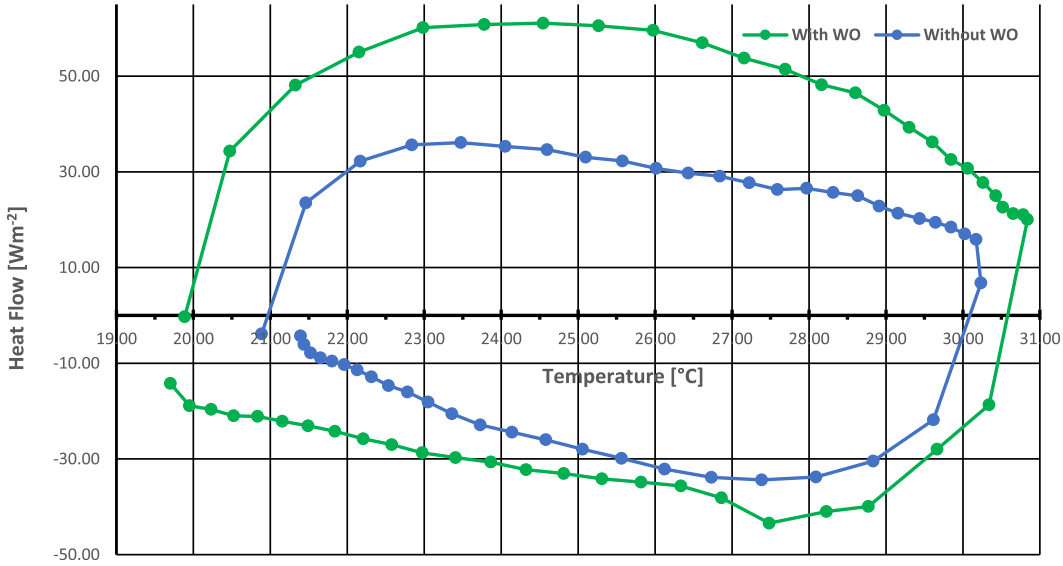

FIGURE 10 Incoming and outcoming heat flow differences with respect to the mean panel temperature in the cycle n. 2.

Cycle n. 2 (see Figure 10), which highlighted the higher difference between incoming and outcoming heat flow, was thoroughly analyzed to better describe the variation of the difference between incoming and outcoming heat flow through the panels, to the variation of panel mean temperature. The heat flow changed direction and sign according to the heating or cooling cycle phase, for each temperature value. Two different values of heat flow were reported: one when the heater was turned on (charge phase) and the other one when the heater was turned off (discharge phase).

4 | DISCUSSION

The thermal conductance values obtained for the two panels from the different methods are quite similar, although the average conductance of the panel with WO (equal to 4.07 $W\,m^{-2}\,K^{-1}$) resulted in a slightly higher (i.e., 6.8%) than the conductance of the panel without WO (i.e., 3.81 $W\,m^{-2}\,K^{-1}$). The major thermal conductance level is due to the higher conductance of the WO inside the canes. The WO in the canes has higher conductance than when the canes are empty. The values of thermal conductance obtained for this panel typology provide the values of thermal conductivity $\lambda_{GC} = 0.19\,W\,m^{-1}\,K^{-1}$ and $\lambda_{GCO} = 0.20\,W\,m^{-1}\,K^{-1}$, respectively, for the panel without WO and with WO. These values have the same order of magnitude of commercial masonry empty block, ranging around the values from 0.18 to 0.25 $W\,m^{-1}\,K^{-1}$ declared from different producers. On the other hand, the thermal conductivity values of the present panel are very similar to those provided by[21] reporting values about 0.12–0.15 $W\,m^{-1}\,K^{-1}$ for insulation panels filled with corn cobs. Finally, just to provide a more general view, the values provided in this paper, following the outcomes of Schiavoni et al.,[41] are very similar to those currently observed in past experimental tests adopting other natural materials from biomass as insulation materials.

The heat flow analysis showed a different behavior between the panel without WO and the panel with WO. The heat flow data analysis of the panel with WO, highlighted more constant thermal behavior, with regular cycles and with the same amplitudes. The high heat loss highlighted by the data analysis of the panel with WO in Figure 7 and evaluated with (6) and (7) is very informative. The high heat loss is mainly due to the envelope thermal dispersion of the PASLINK and to the imperfect unidirectionality of the heat flow. In fact, the canes full of WO, with higher thermal conductance, redirect the heat flow parallel to the panel surfaces, limiting the perpendicular heat flow. The panel with WO, during the first phase, absorbs higher incoming heat than the panel without WO. The heat flow absorbed by the panel is almost constant in the temperature range of 23–26°C (Figure 10). The maximum value of heat flow absorbed was 61.08 Wm^{-2} around a mean panel temperature of 24°C, corresponding to a melting temperature range of the WO, this is highlighted in Figure 9 also. It is very interesting to note that for the candelilla e BW combination choice for the WO utilized, the T_{on} temperature (T_{on} represents the temperature below which the WO is solid) is 22.45°C, and the T_p temperature (T_p represents the peak maximum temperature, above which the crystals are liquid) is about 31.09°C. The panel without WO at the same temperature of 24°C absorbed an incoming heat flow of 34.64 Wm^{-2} which is about 57% of the panel with WO. The panel with WO released at a temperature of about 27.5°C, a heat flow of 43.42 Wm^{-2}. At the same temperature of about 27.5°C, the panel without WO released a heat flow of 34.38 Wm^{-2} which is about 80% that of the panel with WO.

5 | CONCLUSIONS

A lot of modern novel bio-based building solutions are derived from traditional architecture. This is characterized by the use of local materials often based on vegetal resources such as wood, straw, and hemp, often agricultural residual raw materials with low inside content energy. Historically, these solutions highlighted good performance value, which has been handed down as the benchmark.[36] However, it is important to improve the solution performance and to adapt them to modern architecture. To achieve these goals, it is necessary

to study and analyze the outcomes of the solutions in use, to improve performance and to ensure efficient and effective application. In these last few years, different studies and research projects were carried out in this field and a lot of bio-based building solutions have been proposed. This is evidenced by many government actions aiming at improving bio-based solutions, with the European Green New Deal being an example. It is necessary to revitalize traditional solutions for enhancing and improving them but with particular attention to maintaining their environmental sustainability.

The building solution proposed in this paper responds to these criteria, it allows to improve the original performance of a traditional wall solution diffused in the rural Mediterranean architecture, based on the utilization of thin panels of A.d. and gypsum, cheap materials largely available in this area. The addition of a natural WO made with soybean oil, BW, and candelilla, has enhanced the thermal capacity of the panel. A specific experimental campaign, aiming at the comparison of traditional and innovative panels, was carried out to assess the enhanced thermal performance of the proposed solution. For a temperature of 27°C, the maximum value of heat flow absorbed from the panel with WO was 61.08 Wm^{-2} whereas the panel without WO absorbed an incoming heat flow of 34.64 Wm^{-2}, that is, 57% of the panel with oleogel. The panel with oleogel released a heat flow of 43.42 Wm^{-2} and the panel without oleogel released a heat flow of 34.38 Wm^{-2} which is about 80% of the panel with oleogel. The results highlighted that the addition of natural WO has enhanced the thermal capacity of the panel facilitating heat dissipation.

This paper further proves the A.d. could be a viable and profitable material for insulating applications and encourages future studies on this bio-based by-product. Future studies will investigate practical applications and will consider and assess the durability, fire resistance, sound insulation, and the development of new building components based on the panel proposed in this work.

CONFLICT OF INTEREST STATEMENT

The authors declare no conflict of interest.

DATA AVAILABILITY STATEMENT

The data that support the findings of this study are available from the corresponding author upon reasonable request.

ORCID

Francesco Barreca http://orcid.org/0000-0002-2149-6514

REFERENCES

1. Global Alliance. Global Status Report. 2020.
2. Fetting C. *The European Green Deal, ESDN Report*. ESDN Office; 2020.
3. DESA. World Population Prospects 2022: Summary of Results Ten key messages. *United Nations, Department of Economic and Social Affairs, Population Division* 2022: 2-3.
4. Hu M, Zhang K, Nguyen Q, Tasdizen T. The effects of passive design on indoor thermal comfort and energy savings for residential buildings in hot climates: a systematic review. *Urban Clim*. 2023;49:101466. doi:10.1016/j.uclim.2023.101466
5. Bruno R, Arcuri N, Carpino C. The passive house in Mediterranean area: parametric analysis and dynamic simulation of the thermal behaviour of an innovative prototype. *Energy Procedia*. 2015;82:533-539. doi:10.1016/j.egypro.2015.11.866

6. European Commission. *Development and implementation of initiatives fostering investment and innovation in construction and demolition waste recycling infrastructure*. 2018.
7. GlobalABC, IEA, UNEP. *GlobalABC Roadmap for Buildings and Construction 2020–2050*. 2020.
8. United Nations. *Global Status report for Buildings and Construction 2021*. 2021.
9. Ameen RFM, Mourshed M, Li H. A critical review of environmental assessment tools for sustainable urban design. *Environ Impact Assess Rev*. 2015;55:110-125. doi:10.1016/j.eiar.2015.07.006
10. Rosso F, Peduzzi A, Diana L, Cascone S, Cecere C. A sustainable approach towards the retrofit of the public housing building stock: energy-architectural experimental and numerical analysis. *Sustainability*. 2021;13(5):2881. doi:10.3390/su13052881
11. Barreca F. Use of giant reed *Arundo donax* L. in rural constructions. *Agric Eng Int CIGR J*. 2012;14(3):46-52.
12. Molari L, Coppolino FS, García JJ. *Arundo donax*: a widespread plant with great potential as sustainable structural material. *Constr Build Mater*. 2021;268:121143. doi:10.1016/j.conbuildmat.2020.121143
13. Rodríguez-Salinas P, Ruiz Morales M, Franco A, Pérez-Fernández AR, Lobato-Calleros O. Efecto de amortiguamiento térmico de una barrera verde de *Arundo donax* como elemento de bioclimatización en edificios. *Inf Constr*. 2017;69:e216.
14. Barreca F, Martinez Gabarron A, Flores Yepes JA, Pastor Pérez JJ. Innovative use of giant reed and cork residues for panels of buildings in Mediterranean area. *Resour Conserv Recycl*. 2019;140:259-266. doi:10.1016/j.resconrec.2018.10.005
15. CABI. Invasive Species Compendium. 2022.
16. Jiménez-Ruiz J, Hardion L, Del Monte JP, Vila B, Santín-Montanyá MI. Monographs on invasive plants in Europe N° 4: *Arundo donax* L. *Bot Lett*. 2021;168(1):131-151. doi:10.1080/23818107.2020.1864470
17. Spencer DF, Colby L, Norris GR. An evaluation of flooding risks associated with giant reed (*Arundo donax*). *J Freshw Ecol*. 2013;28:397-409. doi:10.1080/02705060.2013.769467
18. Hardion L, Verlaque R, Rosato M, Rosselló JA, Vila B. Impact of polyploidy on fertility variation of Mediterranean *Arundo* L. (Poaceae). *C R Biol*. 2015;338(5):298-306. doi:10.1016/J.CRVI.2015.03.013
19. Fichera CR, Barreca F. Performance evaluation of giant reed panels in sustainable agricultural buildings. *Structures and Environmental Technologies International Conference of Agricultural Engineering - Cigr-Ageng 2012: Agriculture and Engineering for a Healthier Life*, Valencia, Spain. 2012.
20. Broadbent G. The ecology of the mudhif. *WIT Trans Ecol Environ*. 2008;113:15-26. doi:10.2495/ARC080021
21. Bovo M, Giani N, Barbaresi A, et al. Contribution to thermal and acoustic characterization of corn cob for bio-based building insulation applications. *Energy Build*. 2022;262:111994. doi:10.1016/J.ENBUILD.2022.111994
22. Zamolyi F, Herbig U. Reed as building material – renaissance of vernacular techniques. Paper presented at: International Symposium on Advanced Methods of Monitoring Reed Habitats. 2010. doi:10.13140/RG.2.2.17343.41120
23. canyaviva.
24. Guillamet GV. *Arundo donax* structures as economic and ecological formworkforfor concrete shells. *Fib Symp*. 2019;72(293):369-376.
25. Winkler-Moser JK, Anderson J, Felker FC, Hwang HS. Physical properties of beeswax, sunflower wax, and candelilla wax mixtures and oleogels. *J Am Oil Chem Soc*. 2019;96(10):1125-1142. doi:10.1002/aocs.12280
26. Meng B, Zhang X, Hua W, Liu L, Ma K. Development and application of phase change material in fresh e-commerce cold chain logistics: a review. *J Energy Storage*. 2022;55:105373. doi:10.1016/J.EST.2022.105373
27. Mishra DK, Bhowmik S, Murari Pandey K. Numerical investigation of beeswax based phase change material for thermal management of Li-ion battery. *Mater Today Proc*. 2021;45(7):6527-6532. doi:10.1016/j.matpr.2020.11.455
28. Kannan KG, Kamatchi R. Augmented heat transfer by hybrid thermosyphon assisted thermal energy storage system for electronic cooling. *J Energy Storage*. 2020;27:101146. doi:10.1016/j.est.2019.101146
29. Huang D, Wang Z, Sheng X, Chen Y. Bio-based MXene hybrid aerogel/paraffin composite phase change materials with superior photo and electrical responses toward solar thermal energy storage. *Sol Energy Mater Sol Cells*. 2023;251:112124. doi:10.1016/J.SOLMAT.2022.112124
30. de Araujo Passos LA, van den Engel P, Baldi S, De Schutter B. Dynamic optimization for minimal HVAC demand with latent heat storage, heat recovery, natural ventilation, and solar shadings. *Energy Convers Manag*. 2023;276:116573. doi:10.1016/J.ENCONMAN.2022.116573

31. Gopi Kannan K, Kamatchi R. Experimental investigation on thermosyphon aid phase change material heat exchanger for electronic cooling applications. *J Energy Storage*. 2021;39:102649. doi:10.1016/j.est.2021.102649
32. Wang X, Li W, Luo Z, Wang K, Shah SP. A critical review on phase change materials (PCM) for sustainable and energy efficient building: design, characteristic, performance and application. *Energy Build*. 2022;260:111923. doi:10.1016/J.ENBUILD.2022.111923
33. Boussaba L, Foufa A, Makhlouf S, Lefebvre G, Royon L. Elaboration and properties of a composite bio-based PCM for an application in building envelopes. *Constr Build Mater*. 2018;185:156-165. doi:10.1016/j.conbuildmat.2018.07.098
34. Blake AI, Marangoni AG. The effect of shear on the microstructure and oil binding capacity of wax crystal networks. *Food Biophys*. 2015;10(4):403-415. doi:10.1007/s11483-015-9398-z
35. Cesaratto PG, De Carli M. A measuring campaign of thermal conductance in situ and possible impacts on net energy demand in buildings. *Energy Build*. 2013;59:29-36. doi:10.1016/j.enbuild.2012.08.036
36. International Standard Organization. ISO 9869-1:2014 Thermal insulation — Building elements — In-situ measurement of thermal resistance and thermal transmittance—Part 1: Heat flow meter method 2014: 36.
37. François A, Ibos L, Feuillet V, Meulemans J. Estimation of the thermal resistance of a building wall with inverse techniques based on rapid active in situ measurements and white-box or ARX black-box models. *Energy Build*. 2020;226:110346. doi:10.1016/j.enbuild.2020.110346
38. Bloem JJ. Workshop on the Application of System Identification in Energy Savings in Buildings. In: Institute for Systems Engineering and Informatics, Joint Research Centre, Ispra 25–27 October 1993. Italy: 1993.
39. Gutschker O. Parameter identification with the software package LORD. *Build Environ*. 2008;43(2):163-169. doi:10.1016/j.buildenv.2006.10.010
40. Ndukwu M, Ibeh M, Ekop I, et al. Analysis of the heat transfer coefficient, thermal effusivity and mathematical modelling of drying kinetics of a partitioned single pass low-cost solar drying of cocoyam chips with economic assessments. *Energies*. 2022;15(12):4457. doi:10.3390/en15124457
41. Schiavoni S, D'Alessandro F, Bianchi F, Asdrubali F. Insulation materials for the building sector: a review and comparative analysis. *Renew Sustain Energy Rev*. 2016;62:988-1011. doi:10.1016/j.rser.2016.05.045

How to cite this article: Barreca F, Cardinali G, Barbaresi A, Bovo M. Bio-based building components: a newly sustainable solution for traditional walls made of *Arundo donax* and gypsum. *Heat Transfer*. 2023;52:5166-5183. doi:10.1002/htj.22921